Tuijin Jishu/Journal of Propulsion Technology
ISSN: 1001-4055
Vol. 45 No. 3 (2024)

Flexural performance of Textile Reinforced Slabs Subjected to Point Load

Nambiyanna.B[1], Kiran S, Manjunath G Y [2]

[1] Assistant Professor, Department of Civil Engineering, Ramaiah Institute of Technology, Bangalore, Karnataka, India,[2] Student, MTech in Structural Engineering, Ramaiah Instittute of Technology.

Abstract: Textile Reinforced Concrete (TRC), type of composite material that combines concrete with high-strength fibre reinforcements like carbon, AR-glass, or basalt fibers. It surpasses traditional steel-reinforced concrete in terms of tensile strength, flexibility, and durability. TRC addresses issues like corrosion and rigidity associated with steel reinforcement, making it ideal for thinner and lighter structural elements. Its unique properties make it suitable for various construction sectors, including load-bearing components, architectural facades, and rehabilitation. TRC supports sustainable construction practices by reducing material usage and enhancing built environment longevity.

It combines the benefits of traditional concrete with strength and flexibility of textile reinforcements. It is composed of fine-grained concrete and high-strength textile fabrics made from materials like carbon, AR-glass, or basalt fibers. It addresses the limitations of conventional steel reinforcement, such as corrosion and limited formability. TRC's superior mechanical properties enable thinner, lighter, and more resilient structural elements, and its applications range from load-bearing structures to infrastructure repair. It also contributes to sustainability by reducing material consumption.

Keywords: *Textile Reinforced Slabs (TRC), Flexural performance, Glass fibre mesh*

1. Introduction

Textile Reinforced Concrete (TRC), it is a special type of material where reinforcement of great strength non-corrosive fabrics consists. Due to this usage of non-corrosive reinforcement, requirement of the cover can be limited to the minimum value. TRC has a higher sustainable potential over normal RC slabs. It is used for the preparation of thin structures like shells etc. Commonly used materials for the textile reinforcement are Glass fibre, Carbon fibre, Boron fibre etc are used for casting purpose (Mansur de Castro Silva & de Andrade Silva, F, 2020). The structures made up of the TR, possesses high strength when compared to conventional RC slabs. The strength to weight ratio of this is high which gives more durability to the structures (Pham, T. M & Hao H, 2016). The improvement in construction materials has been headed to the research of efficient, sustainable structural systems that are incorporated minimum usage of the materials, light weight components and added economical benefits. Textile based material has been studied widely in the past few spans as it is used in the construction field of the new fabricated structural elements and strengthening the existing structural elements by retrofitting process. It can be viewed that one of the most recent solutions such as area of composite materials. The material is said to be innovative as it is based on two components with variable characteristics, and their combination has been driven by the goal of obtaining a composite material with enhanced properties. This material varies conventional steel-reinforced concrete as it includes non-corrosive high performing textiles such as carbon, glass, aramid, or basalt ones. These textiles are embedded into the well grained concrete matrix to confirm that the composite material would be characterized one by enhanced tensional strength and different mechanical characteristics, ductility, and different properties of the non-corrosive textiles with which the material is reinforced (Mansur de Castro Silva & de Andrade Silva F, 2020). It is possible to assume that the use of TR resolves several limitations of dynamics with conventional steel-reinforced concrete since the new material is not susceptible towards corrosion. Tensional strength and the absence of environmental degradation are the key characteristics of textiles used in TRC. As the result, new material has a longer service life and it is used in salty soils, on the seashores, near the chemical facilities, and in other severe conditions. In addition, TRC is lightweight, and the characteristic of this composite is ideal for the bridge construction and other facilities, which should be lightweight.

TRC is a lightweight, non-corrosive alternative to traditional steel-reinforced concrete. Its high-performance textiles, such as carbon, glass, aramid, or basalt fibers, enhance durability and lifespan. TRC is lightweight, allowing for thin, lightweight elements without compromising structural integrity as shown in Figure 1.1. Its high tensional strength improves performance under load and resisting towards cracking. TRC's design flexibility allows for complex shapes, allowing for innovative and aesthetically pleasing structures. TRC elements can be prefabricated off-site, reducing maintenance costs. TRC contributes to sustainable construction practices by reducing the need for heavy steel reinforcements and reducing the amount of concrete required. It also enhances seismic performance, improves load distribution, and can be tailored to specific applications. It also improves thermal insulation and fire resistance (Kim H. Y, et.al, 2020).

2. Experimental Program

2.1 Materials used and Mix proportion

OPC of 53 grade, manufactured sand as fine aggregates, coarse aggregate of 12.5 mm down size, glass fibre mesh are used in construction of concrete specimens. The mix proportion is developed according to the guidelines Specification IS 10262-2009. Table 2.1 indicates the descriptions mix proportion of M25 grade, which were used for casting. Results of a test conducted on the Hardened propertied of M25 has been shown in Table 2.2

Table 2.1: Mix proportion

Materials	Proportions (Kg/m^3)
Cement	435.40
Water	191.58
Fine aggregate	572.27
Coarse aggregate	1204
W/C ratio	0.44

Table 2.2: Hardened properties of M25

Cube Specimen	Test Results N/mm2
1	31.24
2	30.89
3	32.85
AVG	31.66

Slab details is shown in the below Table 2.3

Table 2.3: Slab Details

Sl No	Slab type	L(mm)	B(mm)	T(mm)	Bottom Layer	Top Layer	Middle Strip	Top Strip
1.	TS/BL	1000	480	70	✓			
2.	TS/BL/TLS-1	1000	480	70	✓			✓
3.	TS/BL/TLS-2	1000	480	70	✓			✓✓
4.	TS/BL/TLS-3	1000	480	70	✓			✓✓✓
5.	TS/BL/TL/MS-1	1000	480	70	✓	✓	✓	
6.	TS/BL/TL/MS-2	1000	480	70	✓	✓	✓✓	
7.	TS/BL/TL/MS-3	1000	480	70	✓	✓	✓✓✓	

2.2 Preparation of formwork

Formwork is made up of steel frame as shown in Figure 2.1. The carpentry work is done so that the required size is achieved, the inside surface of steel frame is oiled before casting in order to make demolding easier. A cover was used at the bottom of the formwork above which concrete with glass fibre mesh is placed.

Figure 2.1 Preparation of formwork

2.3 Mixing of concrete and Casting of specimens

Total 7 number of slabs were casted by pouring concrete mix to the steel frame formwork with different configurations of the glass fibre mesh i.e., at the bottom, middle and top. Glass fibre mesh of size (1000×480) mm and the glass fibre strip of size (1000×76.2) mm as shown in the Figure 2.2

Figure 2.2 Total slab cast = 7

2.4 Curing

Curing was performed after 24hours by putting gunny bags and watering it for 28days. Specimens are white washed in order to visualize clear crack pattern.

2.5 Test Setup and Instrumentation

The testing apparatus i.e., UTM that was used for the testing purpose is setup by using 2 mild steel rod of (530 x 50)mm for the support at the base of the slab. 2 rollers of the size (270 x 30) mm is placed at top of the slab for the downward action of the load that acts as a two-point bending load test. The flexural load test was carried out for the determination of the Load-Deflection characteristics, Reinforcement layers confinement, to determine the ductility factor and capacity of energy absorption of the slab and crack pattern characterization of the different slabs under flexural load as shown in the below Figure 2.3. The test machine that was used for testing has a capacity of 100KN. LDVT Digital dial gauge was placed on the slab for deflection measurement.

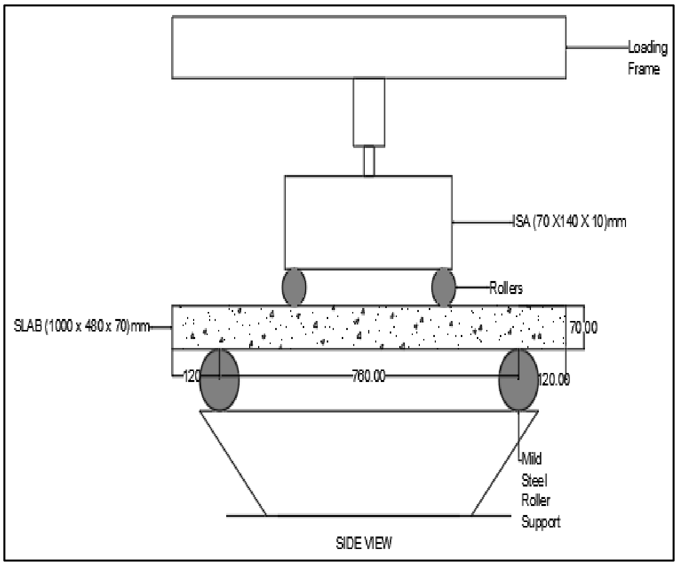

Figure 2.3. CAD draft of Test Setup

Figure 2.4. Universal Testing Machine

3. Results and Discussion

a. Load v/s Deflection response behaviour:

The load response diagram were plotted in order for observing the variation in the middle stage on the ascending part of diagram. This gives the stiffness variation, achievement of peak load and the corresponding deflection will be very useful in identifying deviation among the specimen for better understanding of the slab performance. The load response of each slab and combined load response diagram is plotted in the below figures.

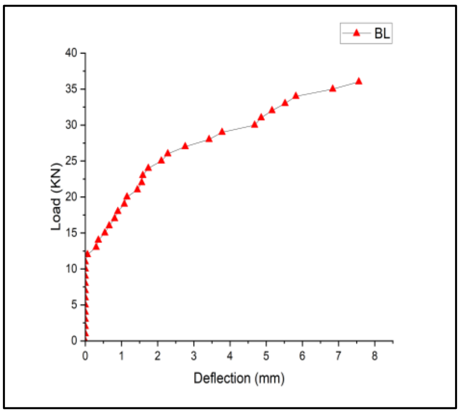

BL Slab

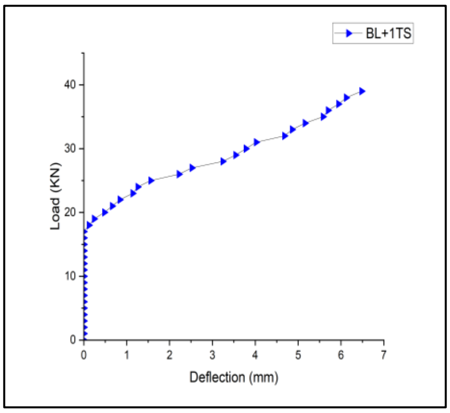

BL + 1TLS

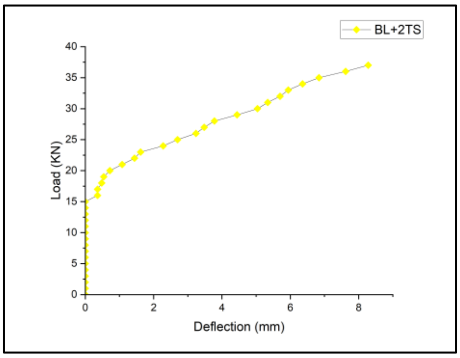

BL +2TLS

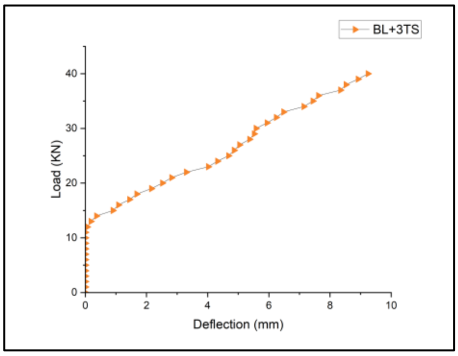

BL + 3TLS

Tuijin Jishu/Journal of Propulsion Technology
ISSN: 1001-4055
Vol. 45 No. 3 (2024)

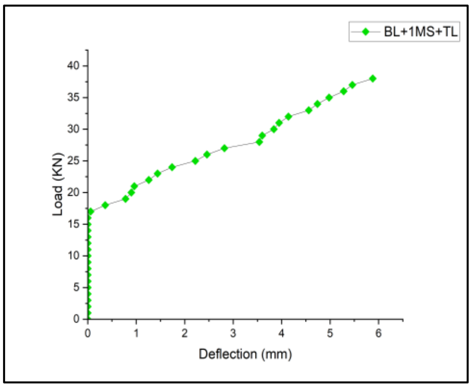

BL + 1MS + TL

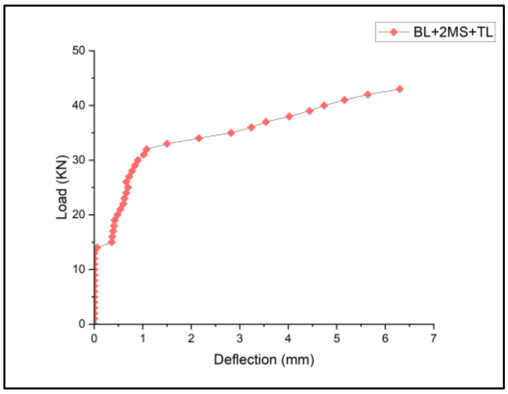

BL + 2MS + TL

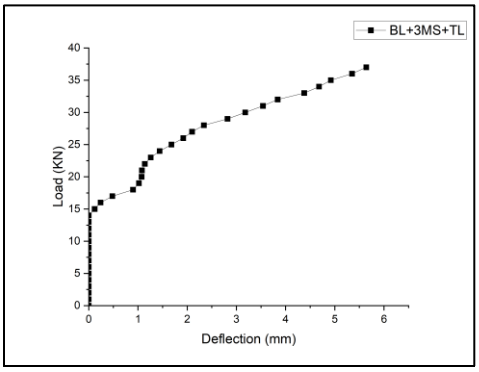

BL + 3MS +TL

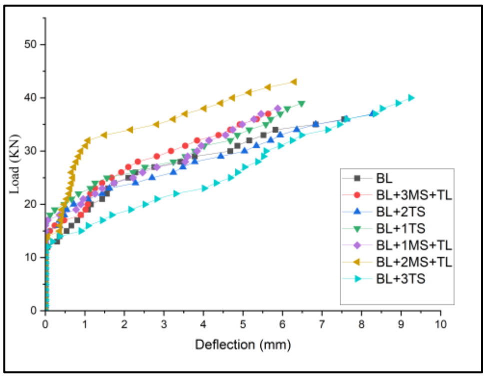

Combined Load v/s Deflection

Visual observations on the load response diagram indicated that Bi-linear behaviour with higher initial stiffness for 3 middle strip and lesser stiffness for 3 top strip is evident. It is evident that, the load response profile of all the specimen were similar up to 32-35% of the ultimate load and from there onwards deviation is observed which indicates the influence of the bonding area and the layers of fibre mesh reinforcement.

b. Deflection Ductility Index

Ductility is a vital parameter regarded in the design of flexural members, generally curvature and deflection ductility are observed for the flexural behaviour to understand the capacity of energy absorption while undergoing large deformations in the post peak stage. It is defined as the ratio of deflection at ultimate load (δ_u) to the deflection at yield load (δ_y) and it is denoted by (μ_d) and curvature ductility is defined as the ratio of curvature at ultimate load to the curvature at the yield load. Identification of the yield point in most of the flexural members is difficult to locate on the load response profile as shown in Figure 3.1

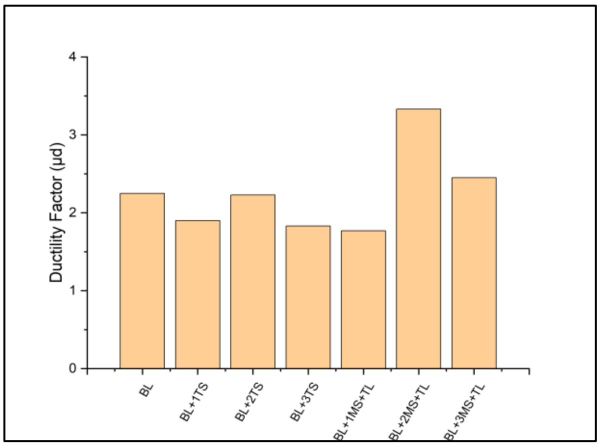

Figure 3.1 Ductility Factor

c. Energy Absorption

The area under the load response profile is represented as total energy absorbed by the specimen. This parameter is also an essential for comparison of performance of the slabs over variable layers of glass mesh. In this section the scope is limited to demonstrate the variation in the energy absorption over the bond area and the spacing of the layers. From the graph we can conclude that the slab having bottom layer, top layer and 2 middle strip absorbs more energy and the slab having bottom layer and 1 top strip absorbs less energy as shown in Figure 3.2

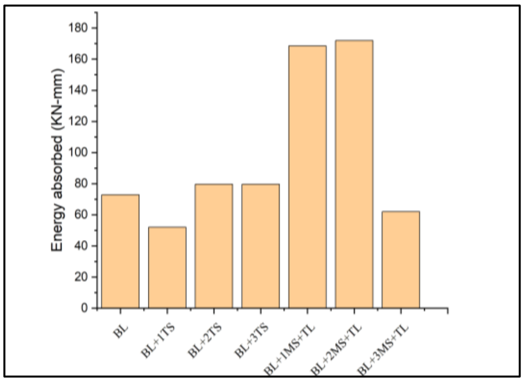

Figure 3.2 Energy Absorption

d. Crack deformation and failure pattern of slabs

Great care was exercised in the handling of specimens and their mounting onto the loading frame. All accessories were thoroughly inspected to ensure perfect contact concerning support, and the LVDT (Linear Variable Differential Transformer) was appropriately positioned. Deformation in the slabs commenced upon the application of load, and the first crack emerged in the middle region. This initial crack progressed from the corner of the top side of the slab towards the centre. With further load increase, the depth of the crack amplified, accompanied by a widening of the crack at the bottom surface. After identifying secondary cracks, which were more prevalent on the sides of the slab, necessary markings were made for documentation. Towards the conclusion of the test, the secondary cracks widened in the middle region, while in the side edge region a diagonal crack emerged, leading to the failure of the slab. Visual observations indicated that most cracks were converging toward a focal point, specifically the bottom side of the slab. Throughout each load increment, deformations, crack formation, and then marking were consistently monitored until the slab failed. It was detected that, all slabs failed in the amended middle region. In following figures, snapshot clearly depicts the marked crack profile, organized in descending order based on the bond area and the layers of glass mesh fibre as shown in the below figures.

BL BL + 1TLS BL + 2TLS

BL + 3TLS

BL + 1MS +TL

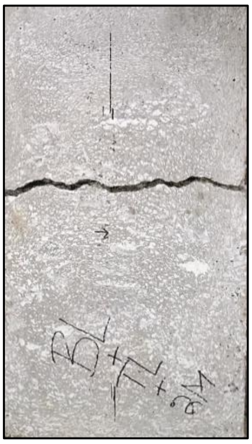

BL +2MS +TL

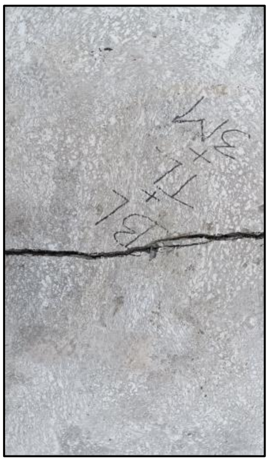

BL +3MS +TL

Based on the preliminary study and the test that was conducted, it has been observed that the slabs which has been undergone bending test, the cracks were initially generated at the middle section of the slab at the load above 12-15KN based on the layers of the glass fibre mesh. After attaining the peak load and maximum deflection the slabs were failed because of the brittle nature of the mesh. Each slabs with cracking patterns is shown above Chinnasamy, M., Ajithkumar, et. al (2020)

4. Conclusions

The study analysed the load versus deflection response of textile-reinforced slabs, revealing a bi-linear behaviour across all specimens. Initial stiffness was higher in slabs with three middle strips compared to those with three top strips. Load response consistency was uniform up to 32-35% of ultimate load, but deviations became evident beyond this point due to variations in bonding area and reinforcement layer configuration. The study confirms the significant role of reinforcement configuration in influencing bearing capacity, underscoring the importance of detailed design considerations for optimizing structural performance. The configuration of fiber mesh layers significantly affects the bearing capacity. The study emphasizes the importance of reinforcement layout for optimizing structural performance.

In the study of the deflection ductility index (μd) of textile reinforced slabs under point load, key parameters such as the deflection at ultimate load (δu) and deflection at yield load (δy) were critically evaluated. The deflection ductility index provides insight into the capacity of these slabs to undergo large deformations, a crucial factor for assessing energy absorption capabilities in post-peak load scenarios. It was found that the slabs with a combination of bottom and top layers, along with two middle strips, demonstrated the highest deflection ductility index, indicating superior energy absorption and resilience to deformation. Conversely, slabs with only a bottom layer and one top strip exhibited the lowest index, reflecting reduced ductility and energy absorption potential. The adoption of the bilinear method to determine yield points further clarified the relationship between load and deflection, establishing a basis for comparative analysis across different slab configurations.

The study on energy absorption in textile-reinforced slabs subjected to point loads revealed significant findings. The investigation focused on various slab configurations, particularly analysing the effects of different layers of glass mesh reinforcement. It was observed that slabs with a combination of bottom, top, and two middle strips exhibited the highest energy absorption capacity. This was attributed to the optimal distribution and bonding area provided by the layers, enhancing the slab's ability to dissipate energy under loading. In contrast, slabs with only a bottom layer and one top strip showed the least energy absorption, indicating the crucial role of adequate layering in achieving better performance. These findings underscore the importance of carefully designing the reinforcement layout to maximize energy absorption, especially in applications requiring enhanced durability and resistance to impacts.

During testing of the slabs, meticulous care was taken to ensure proper handling and mounting onto the loading frame, with thorough inspections of all accessories to guarantee perfect contact during support. The application of load initiated deformation in the slabs, with the first crack appearing in the middle region, progressing from the corner of the top side towards the center. As the load increased, the crack deepened and widened at the bottom surface, leading to the emergence of secondary cracks, particularly on the sides of the slab. Markings were made for documentation as these secondary cracks developed, with the final stages of testing revealing that the secondary cracks widened in the middle region, while diagonal cracks appeared in the side edge region, ultimately leading to slab failure. Observations indicated that most cracks converged towards a focal point on bottom side of the slab. Throughout the load increments, continuous monitoring of deformations, crack formation, and subsequent markings was conducted until the slabs failed, with all specimens exhibiting failure in the amended middle region. The documented crack profiles were organized in descending order based on the bond area and the layers of glass mesh fiber, highlighting the impact of these factors on the cracking behaviour and overall performance of the slabs.

Acknowledgements: We sincerely acknowledge the support of Department of Civil Engineering, Ramaiah Institute of Technology Bangalore for the support extended during this investigation.

Author contributions: All authors contributed to the study conception and design. Material preparation, data collection and analysis were performed by [KS], [MGY], [NB]. The first draft of the manuscript was written by [KS] and all authors commented on previous versions of the manuscript. All authors read and approved the final manuscript.

Declarations:

Conflict of interest "On behalf of all authors, the corresponding author states that there is no conflict of interest".

5. References

[1] Alrshoudi, F. (2021). Textile-reinforced concrete versus steel-reinforced concrete in flexural performance of full-scale concrete beams. *Crystals*, *11*(11), 1272.

[2] Batarlar, B., & Saatci, S. (2022, July). Numerical investigation on the behavior of reinforced concrete slabs strengthened with carbon fiber textile reinforcement under impact loads. In *Structures* (Vol. 41, pp. 1164-1177). Elsevier.

[3] Bernardo, L. F. A., & Lopes, S. M. R. (2003). Flexural ductility of high-strength concrete beams. *Structural Concrete*, *4*(3), 135-154.

[4] Deng, Z., Xia, Q., Gong, M., & Xu, J. (2023). Flexural Strengthening of Two-Way RC Slabs with Textile Reinforced Mortar: Experimental Study and Calculation Model. *KSCE Journal of Civil Engineering*, *27*(12), 5268-5280.

[5] Dong, Z., Deng, M., Dai, J., & Song, S. (2021). Flexural strengthening of RC slabs using textile reinforced mortar improved with short PVA fibers. *Construction and Building Materials*, *304*, 124613.

[6] El-Enein, H. A., Azimi, H., Sennah, K., & Ghrib, F. (2014). Flexural strengthening of reinforced concrete slab–column connection using CFRP sheets. *Construction and Building Materials*, *57*, 126-137.

[7] Gopinath, S., Prakash, A., & Ahmed, A. F. (2020). Flexural impact response and energy absorption characteristics of textile reinforced mortar. *Construction and Building Materials*, *262*, 120630.

[8] Hegger, J., & Voss, S. (2008). Investigations on the bearing behaviour and application potential of textile reinforced concrete. *Engineering structures*, *30*(7), 2050-2056.

[9] Holler, S., Butenweg, C., Noh, S. Y., & Meskouris, K. (2004). Computational model of textile-reinforced concrete structures. *Computers & structures*, *82*(23-26), 1971-1979.

[10] Ibrahim, A. M., Abd, S. M., Hussein, O. H., Tayeh, B. A., Najm, H. M., & Qaidi, S. (2022). Influence of adding short carbon fibers on the flexural behavior of textile-reinforced concrete one-way slab. *Case Studies in Construction Materials*, *17*, e01601.

[11] Kamani, R., Kamali Dolatabadi, M., & Jeddi, A. A. (2018). Flexural design of textile-reinforced concrete (TRC) using warp-knitted fabric with improving fiber performance index (FPI). *The Journal of The Textile Institute*, *109*(4), 492-500.

[12] Karadis, A., Cetin, K., Altıok, T. Y., & Demir, A. (2021). Investigation bending behaviors of the slabs with glass fiber reinforced polymer composite and steel bars. *Journal of Structural Engineering*, *4*(4), 227-238.

[13] Kim, H. Y., Koh, K. T., You, Y. J., Ryu, G. S., Seo, D. W., Jin, S. S., ... & Nam, J. H. (2020). Load-deflection behaviour of concrete slab-type elements casted on stay-in-place TRC formwork. *Composite Structures*, *244*, 112310.

[14] Koutas, L. N., Tetta, Z., Bournas, D. A., & Triantafillou, T. C. (2019). Strengthening of concrete structures with textile reinforced mortars: State-of-the-art review. *Journal of Composites for Construction*, *23*(1), 03118001.

[15] Mansur de Castro Silva, R., & de Andrade Silva, F. (2020). Carbon textile reinforced concrete: Materials and structural analysis. *Materials and Structures*, 53(1), 17.

[16] Petre, D., & Zapalowicz, I. (2012). Analysis of reinforced concrete slabs strengthened with textile reinforcement, *non-linear finite element analysis*.

[17] Pham, T. M., & Hao, H. (2016, August). Review of concrete structures strengthened with FRP against impact loading. In *Structures* (Vol. 7, pp. 59-70). Elsevier.

[18] Preinstorfer, P., Yanik, S., Kirnbauer, J., Lees, J. M., & Robisson, A. (2023). Cracking behaviour of textile-reinforced concrete with varying concrete cover and textile surface finish. *Composite Structures*, *312*, 116859.

[19] Reissen, K., & Hegger, J. (2014, June). Shear strengthening of bridge deck slabs with textile reinforced concrete. In *Proceedings of the 1st Concrete Innovation Conference (CIC), Oslo, Norway* (pp. 11-13).

[20] Schladitz, F., Frenzel, M., Ehlig, D., & Curbach, M. (2012). Bending load capacity of reinforced concrete slabs strengthened with textile reinforced concrete. *Engineering structures*, *40*, 317-326.

[21] Sciegaj, A., Almfeldt, S., Larsson, F., & Lundgren, K. (2023). Textile reinforced concrete members subjected to tension, bending, and in-plane loads: Experimental study and numerical analyses. *Construction and Building Materials*, *408*, 133762.

[22] Valeri, P., Ruiz, M. F., & Muttoni, A. (2020). Modelling of textile reinforced concrete in bending and shear with elastic-cracked stress fields. *Engineering Structures*, *215*, 110664.

[23] Valeri, P., Ruiz, M. F., & Muttoni, A. (2020). Tensile response of textile reinforced concrete. *Construction and Building Materials*, *258*, 119517.

[24] Venigalla, S. G., Nabilah, A. B., Mohd Nasir, N. A., Safiee, N. A., & Abd Aziz, F. N. A. (2022). Textile-reinforced concrete as a structural member: a review. *Buildings*, *12*(4), 474.

[25] Williams Portal, N., Nyholm Thrane, L., & Lundgren, K. (2017). Flexural behaviour of textile reinforced concrete composites: Experimental and numerical evaluation. *Materials and Structures*, *50*, 1-14.

[26] Zdanowicz, K., & Marx, S. (2022). Flexural behaviour of thin textile reinforced concrete slabs enhanced by chemical prestressing. *Engineering structures*, *256*, 113946.

IS Codes referred:

[1] IS 456:2000 PLAIN AND REINFORCED CONCRETE - CODE OF PRACTICE (Fourth Revision)

[2] IS 269 ORDINARY PORTLAND CEMENT, 53 GRADE — SPECIFICATION (First Revision)

[3] IS 383 SPECIFICATION FOR COARSE AND FINE AGGREGATES FROM NATURAL SOURCES FOR CONCRETE (Second Revision)

[4] IS: 4031(Part-11)-1988 METHODS OF PHYSICAL TESTS FOR HYDRAULIC CEMENT PART II DETERMINATION OF DENSITY (First Revision)

[5] IS: 2386(Part-3)-1963 METHODS OF TEST FOR AGGREGATES FOR CQNCRETE PART Ill SPECIFIC GRAVITY, DENSITY, VOIDS‘, ABSORPTldN AND BULKING (Eighth Reprint MARCH 1997)

[6] IS 10262:2019 CONCRETE MIX PROPORTIONING - GUIDELINES (First Revision)